

UNCERTAINTY-BASED MICROMECHANICAL MODELLING OF BAMBOO FIBER-REINFORCED COMPOSITES

Bisheh, H^{1*}, Trujillo, E², Osorio, L², and Abdin, Y¹

¹ Composites Research Network, Department of Materials Engineering, The University of British Columbia, Vancouver, Canada

² Department of Mechanics and Production, Autonomous University of Manizales, Caldas, Colombia

* Corresponding author (Hossein.Bisheh@ubc.ca)

Keywords: *Bamboo fibrous composite, Representative Volume Element, Uncertainty*

ABSTRACT

Design and optimization of composites based on the experimental data are invaluable and costly. Rapid progress in simulation and virtual modelling of composite materials under various loading and boundary conditions is beneficial in the design and development of novel composite materials by examining various realistic scenarios. This paper presents a virtual framework to obtain elastic properties of continuous bamboo fiber unidirectional (UD) composites based on the micromechanical modelling approach. The virtual framework includes the generation of stochastic representative volume elements (RVEs) taking into account the uncertainty and variability in geometry and properties of the bio-based bamboo fibers. The developed models are validated with detailed experimental characterizations and theoretical models. Different realizations of fiber distribution are compared in the assessment of the elastic properties. All modelling and loading scenarios are applied automatically through the python scripting in Abaqus. Uncertainty analysis of input parameters is carried out through parametric studies. This virtual framework can be representative of a real-case model without the need for realistic experiments and therefore can be used in future macromechanical modelling of bamboo fiber-reinforced composites under damage and fatigue conditions.

1 INTRODUCTION

Synthetic fiber-reinforced composites are widely used in various applications from structural to functional applications. However, synthetic fibers such as carbon, glass, and ceramics are not biodegradable and environmentally friendly. Due to the limitations of synthetic fibers and obligations to reduce environmental pollution, producing decomposable composite materials from natural fibers captured the attention of many researchers. Natural fibers can be considered an alternative to synthetic fibers because of their outstanding properties like biodegradability, renewability, lightweight, low cost, abundant availability, low energy requirements, high elastic modulus, and high strength [1,2]. Natural fibers can be extracted from natural plants such as jute, sisal, kenaf, flax, and bamboo which are naturally grown materials and biodegradable after end-of-life [3,4]. Among natural fibers, bamboo fiber has taken much attention because of its high stiffness, high strength, low density, and abundantly available due to fast growth in the nature [5].

To determine the material properties of natural bamboo fiber, experiments are required to extract the data. Although invaluable data can be obtained from real experiments to determine the mechanical properties of natural fiber-reinforced polymer composites, such experiments are limited by cost, complexity and inability to replicate physically some experiments. Recent advances in computational modelling and rapid progress in computer powers have enabled researchers to simulate composite materials and structures from atomic length scale to macroscale

to determine the properties and predict damages and fractures at any scale. Hence, to calculate the elastic properties of bamboo fiber-reinforced composites, a virtual framework simulating the real experiments can be beneficial by reducing the costs and saving time. In computational modelling, various loading scenarios and boundary conditions can be tested to obtain all possible elastic behaviors and the effective elastic properties of composite materials in all directions.

Many researchers utilized computational modelling based on the finite element method (FEM) in their studies to predict elastic properties of composite materials [6–10]. Although there are abundant research studies on elastic responses of synthetic fiber-reinforced composites using micromechanical modelling, limited works in the literature have been dedicated to extract elastic properties of bamboo fiber-reinforced composites through a virtual framework simulating the elastic behaviors using finite element analysis (FEA). Most related research works have used experimental approaches for the mechanical characterization of bamboo fibrous composites [11–14].

Therefore, due to a gap in the literature on micromechanical modelling of bamboo fiber-reinforced composites to derive all possible elastic constants, we have decided to present a research work filling this void. The main novelty and contribution of this study are presenting an algorithm to distribute bamboo fibers in the matrix randomly through uniform and normal random functions as well as considering random radius for the bamboo fibers based on the data obtained from the experiment. Moreover, this paper for the first time contributes a virtual framework through the Python-ABAQUS interface to simulate elastic behaviors of bamboo fiber-reinforced polymer composites by simulating various loading scenarios and boundary conditions.

The methodology presented in this study can construct a 3D model of the RVE with random spatial arrangements of bamboo fibers and stochastic fiber radius and then calculate the effective elastic properties. Furthermore, the presented algorithm is capable to control the volume fraction of fibers by modifying the size of the RVE automatically. In addition, the computed effective elastic constants of bamboo/epoxy composites are compared with those obtained from the experimental tests and different theoretical theories.

2 METHODOLOGY

In this section, a fully automatic algorithm is introduced to simulate elastic responses of unidirectional (UD) bamboo fiber-reinforced composites.

2.1 Geometric Modelling

To analyze a composite material by micromechanics, we need to isolate a 3D RVE from a sample material at macroscale (Figure 1). Hence, the RVE should be a good representative of the whole model including the exact volume fraction of fibers in the matrix. In reality, various fiber distributions in the matrix may occur such as a hexagonal pack of fibers, square distribution, and or random distribution. To have an accurate micromechanics model, random distribution of fibers in the matrix is recommended. In this study, we present an algorithm to distribute bamboo fibers in random positions in an epoxy matrix with a random fiber radius. The proposed algorithm is able to distribute fibers on the boundary (edges and corners) of the RVE as well as inside the RVE. Moreover, a limit for the fiber volume fraction is assumed first and then after random fiber distribution with random radius, the volume fraction is checked to not be more than the limit. As shown in Figure 1, (x, y, z) represents the RVE global cartesian coordinates and $(1,2,3)$ indicate the RVE material principal coordinates where 1- or z-axis is along the fiber longitudinal direction, 2- or x-axis and 3- or y-axis are along with the fiber transverse directions (normal to the fiber longitudinal direction). In this study, for stochastic fiber arrangement in the matrix, a random uniform function is employed. To assign stochastic fiber radius (in the range 40.1303 - 126.2442 μm extracted from the experiments [15]), a random normal function is used.

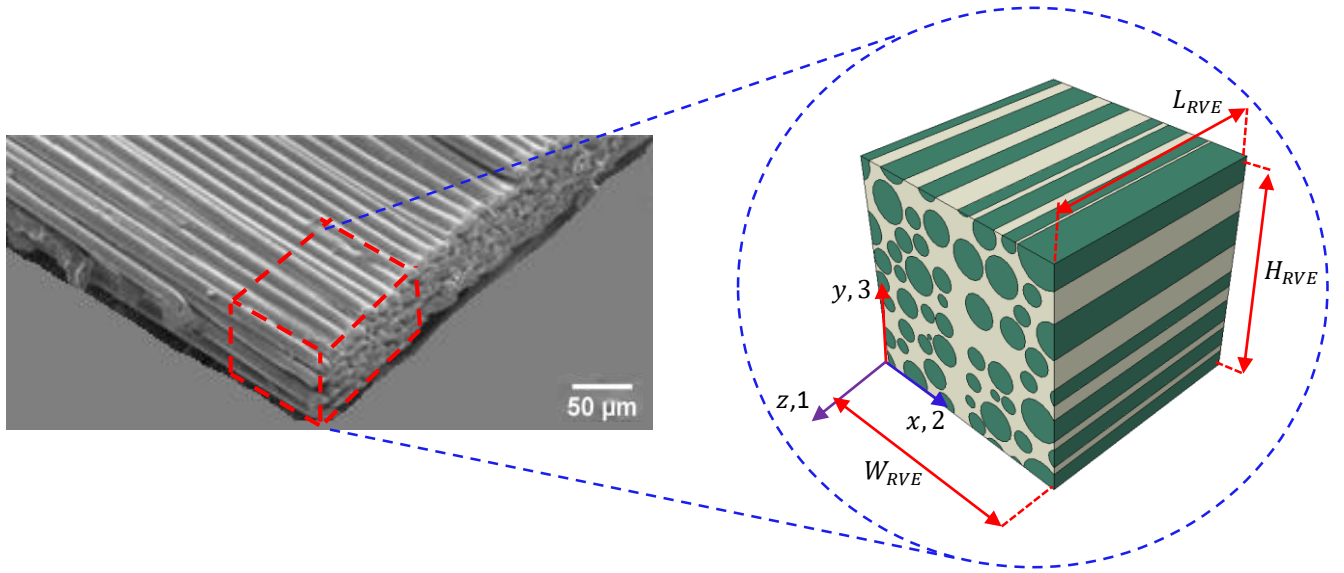


Figure 1. A Representative Volume Element (RVE) of a UD fiber-reinforced composite lamina.

2.2 Generating 3D RVE Model

The developed algorithm is capable to generate 3D RVE models with random distributions of fibers on both inside and the boundary of the RVE with random fiber radius. Inputs of this algorithm are a list of fiber radius, fiber volume fraction (V_f), width (W_{RVE}), height (H_{RVE}), and length (L_{RVE}) of the RVE. For the list of fibers with various radii, the algorithm then finds the minimum and maximum radii (R_{min} and R_{max}) and calculates mean radius (R_{ave}) and standard deviance (STDEV). It should be noted that in the random fiber distribution, various spatial realizations of inclusions will occur after each run of the algorithm for a constant fiber volume fraction.

2.3 Investigating Overlap and Touch of Fibers

Since fibers are randomly distributed within the RVE, there is the possibility of a fiber intersection with other ones. The developed algorithm is able to check and prevent any overlap and contact (or touch) of a fiber with other generated fibers. Figure 2 shows a typical RVE window with origin $(X_{0,RVE}, Y_{0,RVE})$, width W_{RVE} and height H_{RVE} which illustrates how the developed methodology prevents any overlap and touch (or contact) of a fiber with other fibers. Coordinates of top left, top right, and bottom right corners of the RVE are, respectively, $(X_{0,RVE}, Y_{H,RVE})$, $(X_{W,RVE}, Y_{H,RVE})$, and $(X_{W,RVE}, Y_{0,RVE})$.

To prevent the overlap and intersection, the distance d_n between centers of k^{th} fiber with center coordinates (x_k, y_k) and any other fiber n ($n = 1, 2, 3, \dots, k - 1$) with center coordinates (x_n, y_n) in the RVE must be greater than the sum of the radius of fiber k (R_k) and radius of fiber n (R_n) and tolerance or gap between two fibers (see Fig. 2). Hence, based on the Euclidean relationship, the following equation should be satisfied to prevent any overlap and touch between fibers, i.e.

$$d_n = \sqrt{(x_n - x_k)^2 + (y_n - y_k)^2} > R_n + R_k + Tol \quad (1)$$

where gap between fiber k and fiber n is defined as follows [16],

$$Tol = 0.07 \times R_f \quad (2)$$

and R_f is the fiber radius when all distributed fibers have the same radius, and for the case that random fiber radius is distributed according to the list of fiber radius data (which may be obtained from experimental results), R_f may be chosen as the average of all fiber radii.

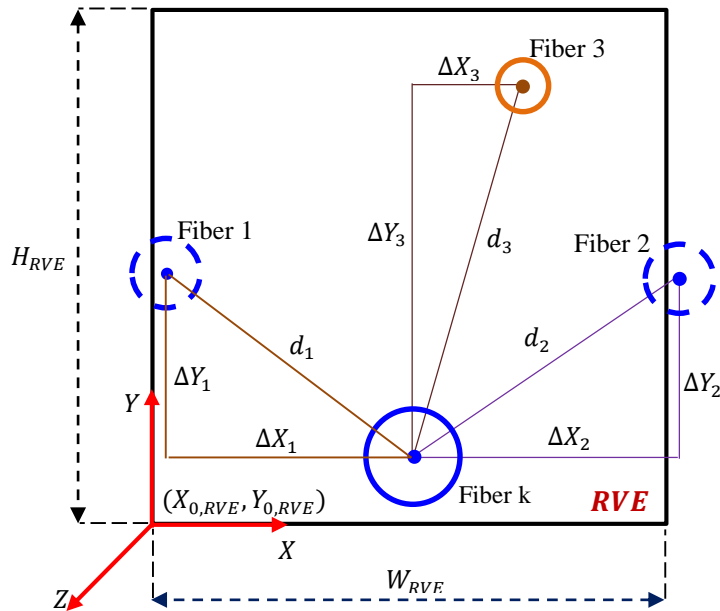


Figure 2. The methodology to prevent fiber overlap and touch in the RVE.

2.4 Creating Periodic Materials

Due to the random distribution of fibers, they may be placed on the boundary of the RVE such as left, right, top, and bottom edges and or on four corners of the RVE. In this case, the sections of fibers which are out of the boundary should be removed and periodic fibers in opposite sides of the master fiber will be generated to keep the fiber volume fraction constant. The developed algorithm in this study is able to check the intersection of fiber k with the RVE boundary and then produce periodic fibers on opposite sides as shown in Figure 3.

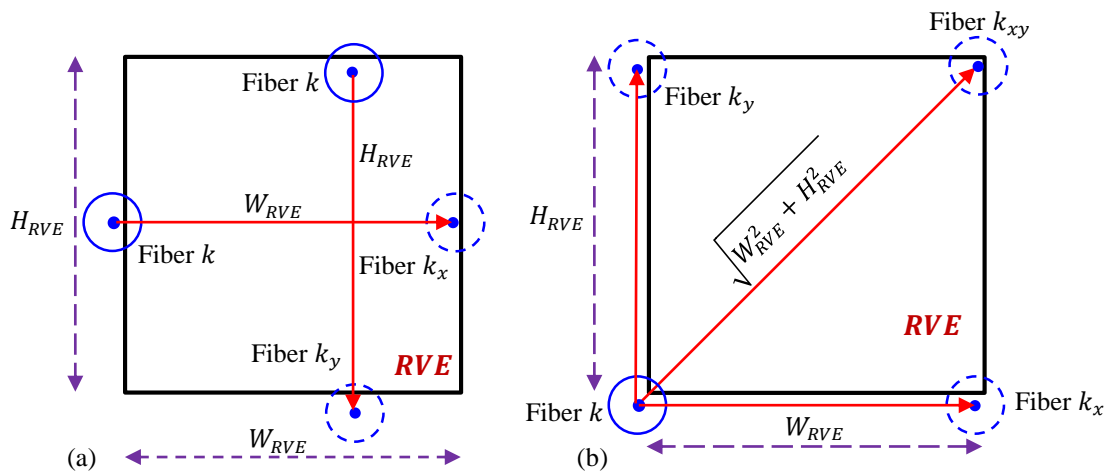


Figure 3. All boundary fiber cases with corresponding periodic fibers.

2.5 Control of Fiber Volume Fraction

The presented algorithm is capable to check and control the fiber volume fraction after generating all fibers. Since, after generating all fibers, especially for random fiber radius, the fiber volume fraction may be higher than the volume fraction limit defined first. The algorithm calculates automatically the fiber volume fraction after creating

each fiber and if it is higher than the limit, it will automatically modify the width and height of the RVE to meet the limit.

2.6 Generating 3D RVE Reinforced with Fibers

After generating center coordinates and radius of all required fibers and the RVE sizes meeting the volume fraction limit, the algorithm through Python scripts creates automatically 3D RVE including all fibers in the corresponding coordinates in ABAQUS CAE software.

2.7 Fiber and Matrix Material Selection

Since, the main objective of this study is to obtain elastic properties of bamboo fiber-reinforced composites through a virtual framework and modelling, bamboo is selected as the fiber material where its properties are listed in Table 1. Bamboo fiber material properties were obtained from experimental tests developed by Trujillo [15]. For the matrix material, epoxy resin Epikote 828 is considered where its material properties are listed in Table 2.

Table 1. Material properties of bamboo fiber [15].

Material	Young's modulus (GPa)	Poisson's ration, ν
Bamboo	43	0.33

Table 2. Material properties of epoxy resin Epikote 828 [15].

Material	Young's modulus (GPa)	Yield stress (MPa)	Poisson's ration, ν
Bamboo	2.7	70	0.35

2.8 Finite Element Mesh Generation

After constructing a 3D RVE model composed of reinforcing bamboo fibers and epoxy matrix, FE mesh is generated over the model to solve it for different elastic constants. To generate finite element mesh, quadratic hexahedral elements of type C3D20R with an edge discretization size of $18\mu m$ are assigned.

2.9 Loading and Boundary Conditions

To obtain all elastic constants of a UD fiber-reinforced composites including three longitudinal and transverse moduli (E_{11}, E_{22}, E_{33}), three shear moduli (G_{12}, G_{13}, G_{23}), and six Poisson's ratios ($\nu_{12}, \nu_{13}, \nu_{21}, \nu_{23}, \nu_{31}, \nu_{32}$), we need to apply appropriate loading and boundary conditions to simulate the real case conditions. Hence, specific loading and boundary scenarios are imposed to construct uniaxial loading cases along x-, y-, and z-axes and shear loading conditions on x-y, y-z, and x-z planes as demonstrated in Tables 3 and 4.

3 RESULTS and DISCUSSION

3.1 Validation

The presented algorithm and methodology are validated and verified through comparison with the existing data in the literature. Hence, the effective elastic properties of a bamboo/epoxy composite computed using the presented algorithm in this study are compared with those obtained from the experimental test or analytical approaches. For the verification purpose, a cubic RVE of $1000\mu m \times 1000\mu m \times 1000\mu m$ with fiber volume fraction of $V_f = 40\%$ is considered. As seen from Table 5, the effective elastic (tensile) modulus in fiber direction (E_{11}) obtained from this study has a good agreement with that obtained from the experimental data of Trujillo [15] and analytical results based on the Rule of Mixtures method, Shear-lag theory, Mori-Tanaka model, and Halpin-Tsai equation.

Table 3. Nodal constraints imposed on the surfaces of the 3D RVE model to create uniaxial deformation along x –, y –, and z –axes.

Loading type	Nodal constraints
Uniaxial deformation along x –axis	Nodes on the right surface (positive yz -surface): $u_x = \delta_{xx}, u_y = u_z = \theta_x = \theta_y = \theta_z = 0$ Nodes on the left surface (negative yz -surface): $u_x = 0, u_y = u_z = \theta_x = \theta_y = \theta_z \neq 0$ Nodes on the back surface (negative xy -surface): $u_z = 0, u_x = u_y = \theta_x = \theta_y = \theta_z \neq 0$ Nodes on the bottom surface (negative xz -surface): $u_y = 0, u_x = u_z = \theta_x = \theta_y = \theta_z \neq 0$
Uniaxial deformation along y –axis	Nodes on the top surface (positive xz -surface): $u_y = \delta_{yy}, u_x = u_z = \theta_x = \theta_y = \theta_z = 0$ Nodes on the left surface (negative yz -surface): $u_x = 0, u_y = u_z = \theta_x = \theta_y = \theta_z \neq 0$ Nodes on the back surface (negative xy -surface): $u_z = 0, u_x = u_y = \theta_x = \theta_y = \theta_z \neq 0$ Nodes on the bottom surface (negative xz -surface): $u_y = 0, u_x = u_z = \theta_x = \theta_y = \theta_z \neq 0$
Uniaxial deformation along z –axis	Nodes on the front surface (positive xy -surface): $u_z = \delta_{zz}, u_x = u_y = \theta_x = \theta_y = \theta_z = 0$ Nodes on the left surface (negative yz -surface): $u_x = 0, u_y = u_z = \theta_x = \theta_y = \theta_z \neq 0$ Nodes on the back surface (negative xy -surface): $u_z = 0, u_x = u_y = \theta_x = \theta_y = \theta_z \neq 0$ Nodes on the bottom surface (negative xz -surface): $u_y = 0, u_x = u_z = \theta_x = \theta_y = \theta_z \neq 0$

Table 4. Nodal constraints imposed on the surfaces of the 3D RVE model to create shear deformation on xy –, yz –, and xz –planes.

Loading type	Nodal constraints
Shear deformation on xy –plane	Nodes on the right surface (positive yz -surface): $u_y = \delta_{yy}, u_x = u_z = \theta_x = \theta_y = \theta_z = 0$ Nodes on the left surface (negative yz -surface): $u_x = u_y = u_z = \theta_x = \theta_y = \theta_z = 0$
Shear deformation on yz –plane	Nodes on the top surface (positive xz -surface): $u_z = -\delta_{zz}, u_x = u_y = \theta_x = \theta_y = \theta_z = 0$ Nodes on the bottom surface (negative xz -surface): $u_x = u_y = u_z = \theta_x = \theta_y = \theta_z = 0$
Shear deformation on xz –plane	Nodes on the front surface (positive xy -surface): $u_x = -\delta_{xx}, u_y = u_z = \theta_x = \theta_y = \theta_z = 0$ Nodes on the back surface (negative xy -surface): $u_x = u_y = u_z = \theta_x = \theta_y = \theta_z = 0$

Table 5. Results for the effective elastic constant E_{11} of bamboo fiber/epoxy composites ($V_f = \%40$) estimated with several models and compared with the results of the presented algorithm in this study.

Elastic constants (GPa)	Experiment [15]	Rule of Mixtures	Shear-lag theory	Mori-Tanaka model	Halpin-Tsai equation	FEA (Present study)
E_{11}	18-19	18.8	18.6	18.9	17.2	18.476

3.2 Uncertainty Analysis

For uncertainty analysis, six spatial realizations of bamboo fibers with random uniform distribution and random normal radii are considered. For each realization, the effective elastic constants of bamboo/epoxy composites are predicted by the presented algorithm in this study. For all realizations, a cubic RVE of $1000\mu m \times 1000\mu m \times 1000\mu m$ with a constant fiber volume fraction of $V_f = 50\%$ and random fiber radius (in the range $40.1303-126.2442\mu m$) is considered. Table 6 lists the predicted elastic constants for six different spatial realizations of bamboo fibers with mean values and standard deviations. Figure 6 displays the mean elastic constants of six fiber spatial realizations with the standard deviation

As shown in Table 6 and Figure 4, the longitudinal elastic modulus E_{11} is not much sensitive to the effect of fiber spatial realization and fiber random radius with low standard deviation, while higher standard deviations are obtained for transverse elastic moduli E_{22} , E_{33} indicating their sensitivity to the random radius and spatial realization of bamboo fibers. Shear elastic modulus G_{13} is sensitive to the arrangement and radius of the inclusion, however, other shear moduli (G_{12} , G_{23}) are not much sensitive with lower standard deviations. It is seen that Poisson’s ratios ν_{12} , ν_{13} are insensitive to the effect of spatial realization and fiber radius with very low standard deviations. However, significant variability of Poisson’s ratios ν_{21} , ν_{23} , ν_{31} , ν_{32} with the bamboo fiber radius and spatial arrangement is observed (see Table 6 and Figure 4).

Highly dependence of transverse and shear moduli to the spatial realizations of bamboo fibers could be related to the displacement of inclusions from their original positions through transverse or rolling/sliding motion. Typical contour plots of six different spatial arrangements of bamboo fibers with random radius are shown in Figure 5 with high-stress regions.

Table 6. Predicted effective elastic constants, the mean and standard deviation for 5 different realizations. Note unit of moduli, E_{ij} and G_{ij} , is GPa for $i, j = 1, 2, 3$.

Elastic constants	Realization number						Mean	Standard deviation
	1	2	3	4	5	6		
E_{11}	22.98545	22.96490	22.90372	22.97343	23.04826	22.86364	22.95657	0.06484
E_{22}	7.41730	7.68512	7.60339	7.77043	7.55948	7.62674	7.61041	0.11949
E_{33}	7.61559	7.60436	7.93534	7.39143	7.55854	7.47645	7.59695	0.18609
G_{12}	2.43606	2.46668	2.44569	2.49672	2.48100	2.48964	2.46930	0.02438
G_{13}	1.95179	1.92770	2.01479	1.87193	1.95261	1.89445	1.93554	0.05026
G_{23}	1.75517	1.80028	1.80298	1.77745	1.83328	1.73710	1.78438	0.03501
ν_{12}	0.33908	0.33860	0.33992	0.33875	0.33779	0.33813	0.33871	0.00075
ν_{13}	0.33767	0.33733	0.33701	0.34056	0.33913	0.33865	0.33839	0.00133
ν_{21}	0.17025	0.09869	0.15577	0.13763	0.09009	0.08521	0.12294	0.03639
ν_{23}	0.37787	0.40795	0.42134	0.39588	0.38920	0.32525	0.38625	0.03345
ν_{31}	0.12799	0.11003	0.13533	0.11936	0.20451	0.11416	0.13523	0.03517
ν_{32}	0.31385	0.32353	0.45845	0.32342	0.44172	0.38317	0.37402	0.06407

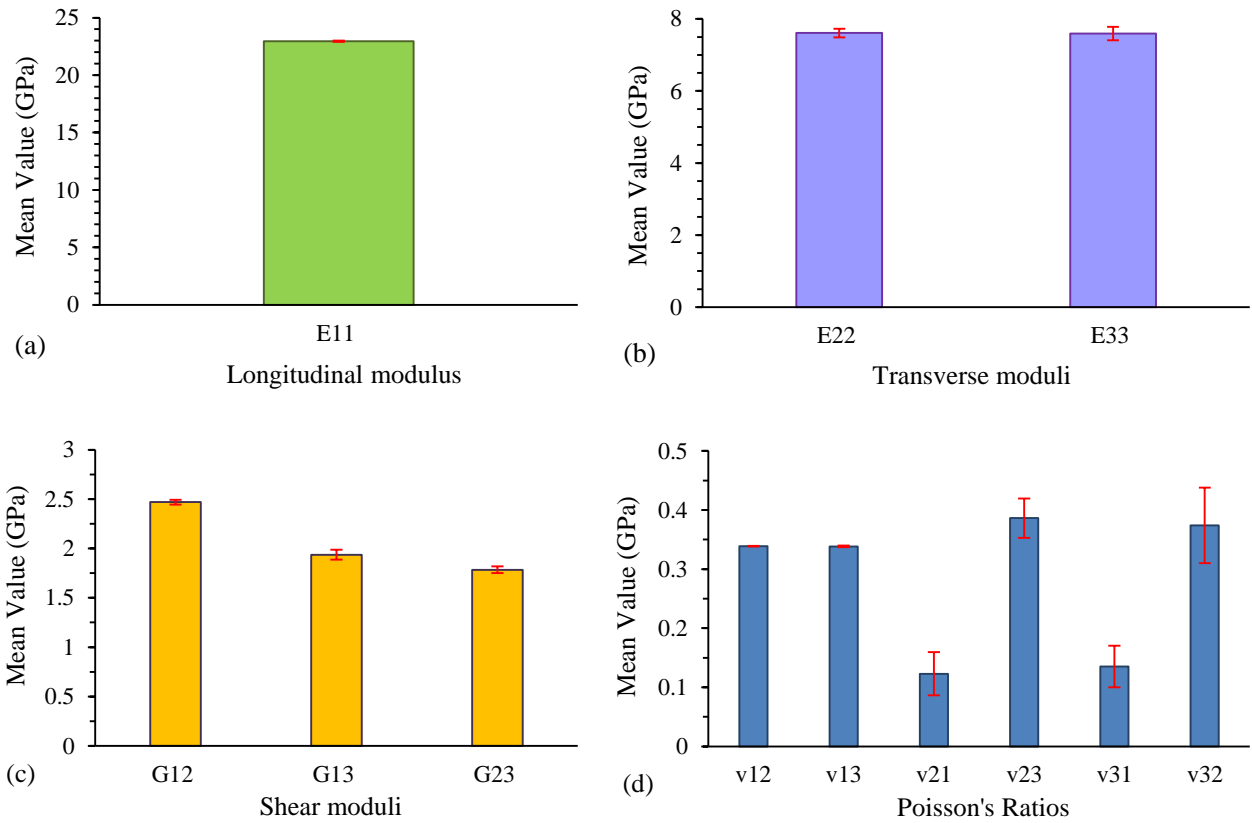


Figure 4. Mean values and standard deviations of elastic constants for six spatial realizations of bamboo fibers in the epoxy matrix.

4 CONCLUSION

This study has presented an algorithm to create a virtual framework to predict elastic constants of bamboo fiber-reinforced composites with random fiber arrangement and radius. The presented approach is capable to distribute fibers on the boundary of the RVE as well as within the RVE. Uncertainty analysis has been performed by calculating the mean and standard deviation of 12 elastic constants for six spatial realizations of inclusions in the matrix. The results demonstrate that some effective elastic properties of bamboo fiber-reinforced composites are dependent on the spatial arrangements and random radius of fibers. The presented algorithm and methodology can construct a virtual test model to simulate elastic behaviors and predict elastic constants of bio-based composites without the need for costly and time-consuming experimental tests.

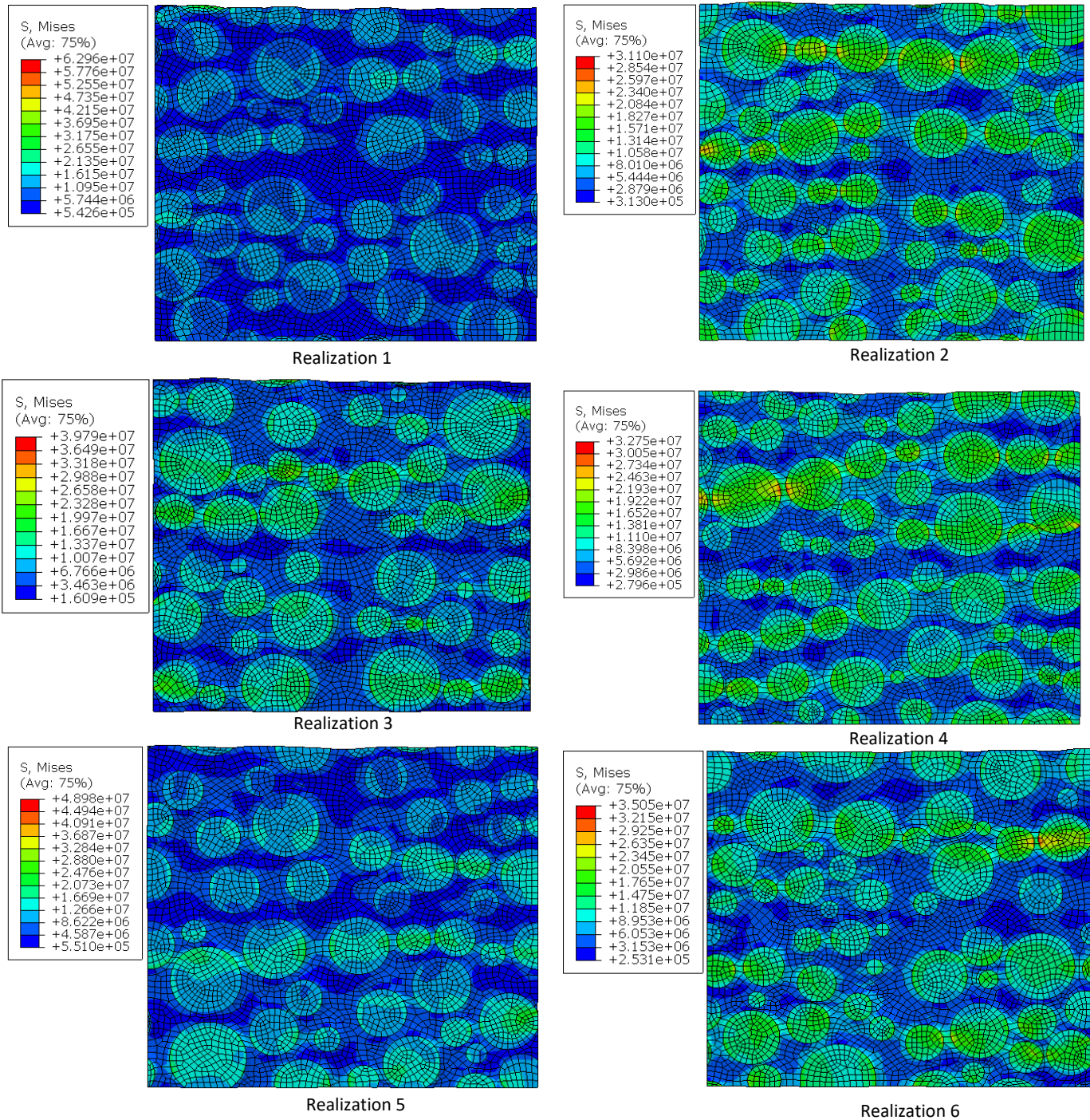


Figure 5. Typical contour plots for transverse uniaxial X-axis deformation for six different spatial realizations of inclusions. All RVEs were imposed with a nominal strain of 0.001.

5 REFERENCES

- [1] S.V. Joshi, L.T. Drzal, A.K. Mohanty, and S. Arora. "Are natural fiber composites environmentally superior to glass fiber reinforced composites?". *Composites Part A: Applied Science and Manufacturing*, Vol. 35, pp 371–376, 2004.
- [2] X. Li, L.G. Tabil, and S. Panigrahi. "Chemical Treatments of Natural Fiber for Use in Natural Fiber-Reinforced Composites: A Review". *J Polym Environ*, Vol. 15, pp 25–33, 2005.
- [3] C. Baley, M. Lan, A. Bourmaud, and A. Le Duigou. "Compressive and tensile behaviour of unidirectional composites reinforced by natural fibres: Influence of fibres (flax and jute), matrix and fibre volume fraction". *Materials Today Communications*, Vol. 16, pp 300–306, 2018.
- [4] P. Pa, and S. M. "Viscoelastic and mechanical behaviour of reduced graphene oxide and zirconium dioxide filled jute/epoxy composites at different temperature conditions". *Materials Today Communications*, Vol. 19, pp 252–261, 2019.
- [5] L. Osorio, E. Trujillo, A.W. Van Vuure, and I. Verpoest. "Morphological aspects and mechanical properties of single bamboo fibers and flexural characterization of bamboo/ epoxy composites". *Journal of Reinforced Plastics and Composites*, Vol. 30, pp 396–408, 2011.
- [6] A.R. Melro, P.P. Camanho, and S.T. Pinho. "Generation of random distribution of fibres in long-fibre reinforced composites". *Composites Science and Technology*, Vol. 68, pp 2092–2102, 2008.
- [7] V. Romanov, S.V. Lomov, Y. Swolfs, S. Orlova, L. Gorbatikh, and I. Verpoest. "Statistical analysis of real and simulated fibre arrangements in unidirectional composites". *Composites Science and Technology*, Vol. 87, pp 126–134, 2013.
- [8] L. Yang, Y. Yan, Z. Ran, and Y. Liu. "A new method for generating random fibre distributions for fibre reinforced composites". *Composites Science and Technology*, Vol. 76, pp 14–20, 2013.
- [9] M.I. Okereke, and A.I. Akpoyomare. "A virtual framework for prediction of full-field elastic response of unidirectional composites". *Computational Materials Science*, Vol. 70, pp 82–99, 2013.
- [10] B. Sabuncuoglu, S. Orlova, L. Gorbatikh, S.V. Lomov, and I. Verpoest. "Micro-scale finite element analysis of stress concentrations in steel fiber composites under transverse loading". *Journal of Composite Materials*, Vol. 49, pp 1057–1069, 2015.
- [11] K. Okubo, T. Fujii, and E.T. Thostenson. "Multi-scale hybrid biocomposite: Processing and mechanical characterization of bamboo fiber reinforced PLA with microfibrillated cellulose". *Composites Part A: Applied Science and Manufacturing*, Vol. 40, pp 469–475, 2009.
- [12] H. Kabir, M.A. Gafur, F. Ahmed, F. Begum, and M.R. Qadir. "Investigation of Physical and Mechanical Properties of Bamboo Fiber and PVC Foam Sheet Composites". *Universal Journal of Materials Science*, Vol. 2, pp 119–124, 2014.
- [13] O. Nurihan, M.R.M. Hisham, Z.A. Rasid, M.Z. Hassan, and A.F.M. Nor. "The elastic properties of unidirectional bamboo fibre reinforced epoxy composites". *International Journal of Recent Technology and Engineering*, Vol. 8, pp 7187–7193, 2019.
- [14] S.C. Chin, K.F. Tee, F.S. Tong, H.R. Ong, and J. Gimbut. "Thermal and mechanical properties of bamboo fiber reinforced composites". *Materials Today Communications*, Vol. 23, 100876, 2020.
- [15] E. TRUJILLO DE LOS RÍOS. "POLYMER COMPOSITE MATERIALS BASED ON BAMBOO FIBRES". Ph.D. Thesis, Katholieke Universiteit Leuven, 2014.
- [16] A.R. Melro. "Analytical and Numerical Modelling of Damage and Fracture of Advanced Composites". Ph.D. Thesis, University of Porto, 2011.